AppliedChem

MDPI

Article

Quantitative Analysis of Formate Production from Plasma-Assisted Electrochemical Reduction of CO_2 on Pd-Based Catalysts

Jie Hu and Fuqiang Liu *

Department of Mechanical & Industrial Engineering, University of Massachusetts Lowell, One University Avenue, Lowell, MA 01854, USA
* Correspondence: fuqiang_liu@uml.edu

Abstract: The escalating levels of atmospheric CO_2, primarily attributed to human activities, underscore the urgent need for innovative solutions to mitigate environmental challenges. This study delves into the electrochemical reduction of CO_2 as a promising avenue for sustainable carbon capture and utilization. Focused on the formation of formate ($HCOO^-$/HCOOH), a high-value product, the research explores the integration of nonthermal plasma (NTP) with electrochemical processes—an approach rarely studied in existing literature. A comprehensive investigation involves varying parameters such as plasma discharging voltage, carrier gas, discharging mode, electrolysis voltage, polarity, and plasma type. The electrochemical tests employ a 10 wt.% Pd/C catalyst, and formate production is quantitatively analyzed using NMR. Results reveal that NTP significantly enhances CO_2 reduction, with key factors influencing formate yield elucidated. The study reveals the complexity of CO_2 electrochemical reduction, providing novel insights into the synergistic effects of NTP. These findings contribute to advancing sustainable technologies for CO_2 utilization, paving the way for more efficient and environmentally friendly processes in the pursuit of a carbon-neutral future.

Keywords: formate; electrochemical CO_2 reduction; plasma; Pd catalyst

Citation: Hu, J.; Liu, F. Quantitative Analysis of Formate Production from Plasma-Assisted Electrochemical Reduction of CO_2 on Pd-Based Catalysts. *AppliedChem* **2024**, *4*, 174–191. https://doi.org/10.3390/appliedchem4020012

Academic Editor: Domenico Osella

Received: 21 January 2024
Revised: 16 March 2024
Accepted: 22 April 2024
Published: 5 May 2024

1. Introduction

CO_2 stands as a notorious greenhouse gas, and human activities, primarily the combustion of fossil fuels, have led to a significant and alarming increase in atmospheric CO_2 concentration over recent decades [1]. To address this environmental challenge, the electrochemical reduction of CO_2 merges as a promising approach for converting CO_2 into valuable products, such as CH_4 [2], C_2H_4 [3], CO [4], $HCOO^-$/HCOOH [5], and CH_3OH [6]. Among all those products, $HCOO^-$/HCOOH is particularly favored due to its relatively high market price, despite its current low production volume [7].

The electrochemical reduction of CO_2 presents a versatile and sustainable solution to the escalating environmental challenges associated with rising CO_2 levels. Over the past decades, the electrochemical reduction of CO_2 into $HCOO^-$/HCOOH with water as the hydrogen source has been extensively investigated by numerous researchers. Early studies of CO_2RR mainly focused on bulk transition and polycrystalline metal-based catalysts, e.g., Pd, Pb, In, Sn, etc. Notably, Pd and Pd-based nanostructures were identified for their efficiency in enhancing formate formation [8]. For instance, Hori et al. reported the use of Pd foil in 0.1 M $KHCO_3$ for electrochemical reduction of CO_2 into formate [9] and achieved a Faradaic efficiency of formate ($FE_{formate}$) formation of 2.8%. Subsequent studies explored catalyst variations, including decorated or supported Pd nanoparticles. Zhao et al. employed Pd nanoparticles decorated on polyaniline-covered MWNTs surfaces (Pd-PANI/CNT) as catalysts for formate production from CO_2RR [10]. An overall 83% of $FE_{formate}$ was reported in their study. Min et al. used Pd/C as the catalyst for synthesizing formate in 0.5 M $KHCO_3$ electrolyte and showed that the Pd nanoparticles loaded

on a carbon-supported electrode demonstrated a great potential for high-mass activities (50~80 mA HCO_2^-) [11]. By switching to Pd-metal-based nanoparticles (Pd NPs), Gao et al. discovered the pathway of CO_2RR to formate on the active phase (α+β PdH_x @PdH_x) of Pd NPs and the $FE_{formate}$ was as high as 90% [12]. Those prior studies suggest that the electrochemical reduction of CO_2 into formate is considerably complicated, involving many factors that are dependent on the catalyst type and structure, composition, catalyst deactivation, reversible evolution of active phases induced by the applied potential, electrolyte type, etc. All these complexities arise from the high inertness of CO_2 and highly sensitive CO_2RR intermediates. However, in the open literature, the studies integrating electrochemical processes and nonthermal plasma in electrochemical CO_2RR are rare.

The impact of nonthermal plasma discharge on electrochemical active surface area and hydrogen adsorption/desorption on Pd catalysts has been investigated in our previous study [13]. In this paper, we systematically studied the use of nonthermal plasma to assist electrochemical reduction of CO_2 towards formate. Specifically, constant-voltage electrochemical CO_2RR tests were conducted, and the produced formate was precisely quantified using NMR. Subsequently, different experimental conditions, including plasma discharging voltage, plasma carrier gas, plasma discharging mode, electrolysis voltage, plasma polarity, and plasma type were explored, and the produced formate was correlated to the test conditions to establish a complete knowledge base of nonthermal plasma-assisted electrochemical CO_2RR. Those results provide a novel insight into the key factors and mechanism in NTP-assisted electrochemical CO_2RR.

2. Materials and Methods

2.1. Materials

The 10 wt.% Pd/C (palladium 10% on carbon, surface area: 1000 m^2/g) was procured from Alfa Aesar Inc. (Haverhill, MA, USA). The 5 wt.% Nafion solution, IPA (99.5%), D_2O (99.9 atom % D), dimethyl sulfoxide (99.9%), and $KHCO_3$ (99.7%) were all sourced from Sigma-Aldrich Inc. (St. Louis, MO, USA). The carbon dioxide was obtained from Airgas (Radnor, PA, USA).

2.2. Preparation of Pd/C Electrodes

To prepare a high-quality working electrode (WE), the glassy-carbon electrode (GCE) was polished using Alpha Alumina (CH Instrument, Inc., Bee Cave, TX, USA) powder with particle sizes of 1.0 μm, 0.3 μm, and 0.05 μm in a sequential manner. After each polishing step, the electrode was thoroughly washed with deionized (DI) water. Subsequently, the electrode was sonicated in a mixed solution of DI water and isopropanol for 3 min.

For investigating the catalyst's effect on formate formation, the catalyst ink was prepared by mixing 20 mg Pd/C (palladium 10% on carbon) in 8 mL DI water, followed by sonication for 15 min. Then, 2 mL IPA (99.5%, Sigma-Aldrich St. Louis, MO, USA) was added to the mixture, and sonication continued for an additional 15 min. A 5 μL catalyst ink was pipetted onto the GCE (3 mm diameter with an electrode area of 7.07 mm^2). Subsequently, 10 μL of Nafion solution (5 wt%, Sigma-Aldrich St. Louis, MO, USA) was dripped onto the GCE after the catalyst was fully dried. The electrode was then transferred to an oven and cured for 30 min at 80 °C.

2.3. Electrochemical Measurements and Product Analysis

All electrochemical experiments were conducted in an H-shaped cell using a Versa 3 Potentiostat (Princeton Applied Research, Nashville, TN, USA). The experimental setup is illustrated in Figure 1. To prevent the transport of chemical species produced by the Pt mesh into the left chamber, a Nafion membrane was employed to partition the H-shaped cell into two parts. In the left chamber (refer to Figure 2), a stainless-steel capillary tube (Varian, Inc., Palo Alto, CA, USA) with an inner diameter of 180 μm was suspended approximately 2 mm above the surface of an aqueous electrolyte. The 3-electrode electrochemical system comprised a working electrode (WE) and a reference electrode (RE) placed in the left

chamber, while the counter electrode (CE) was placed in the right chamber. To minimize the resistance, the WE and RE were positioned as close as possible, considering the critical role of electrolyte internal resistance in CO_2RR.

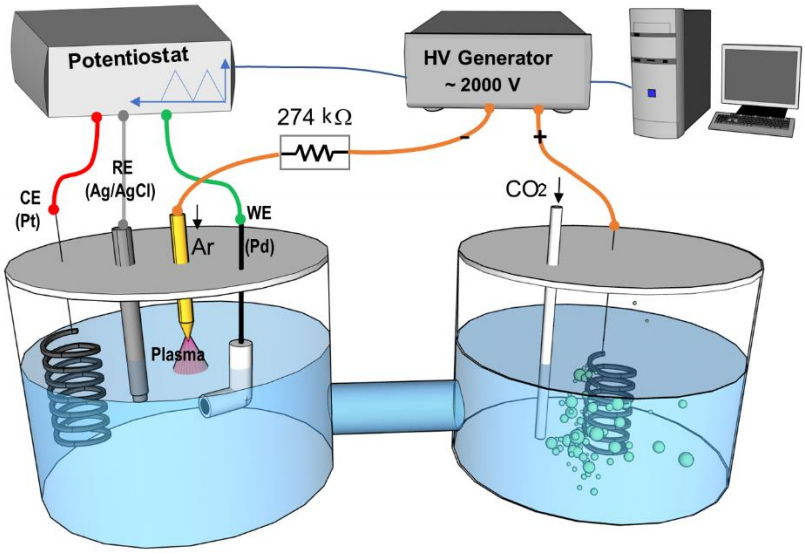

Figure 1. Schematic illustration of the experimental setup. Plasma is formed by a stainless-steel capillary suspended ~2 mm above the surface of an aqueous electrolyte under a negative bias between 1250 and 2500 V relative to a submerged Pt electrode.

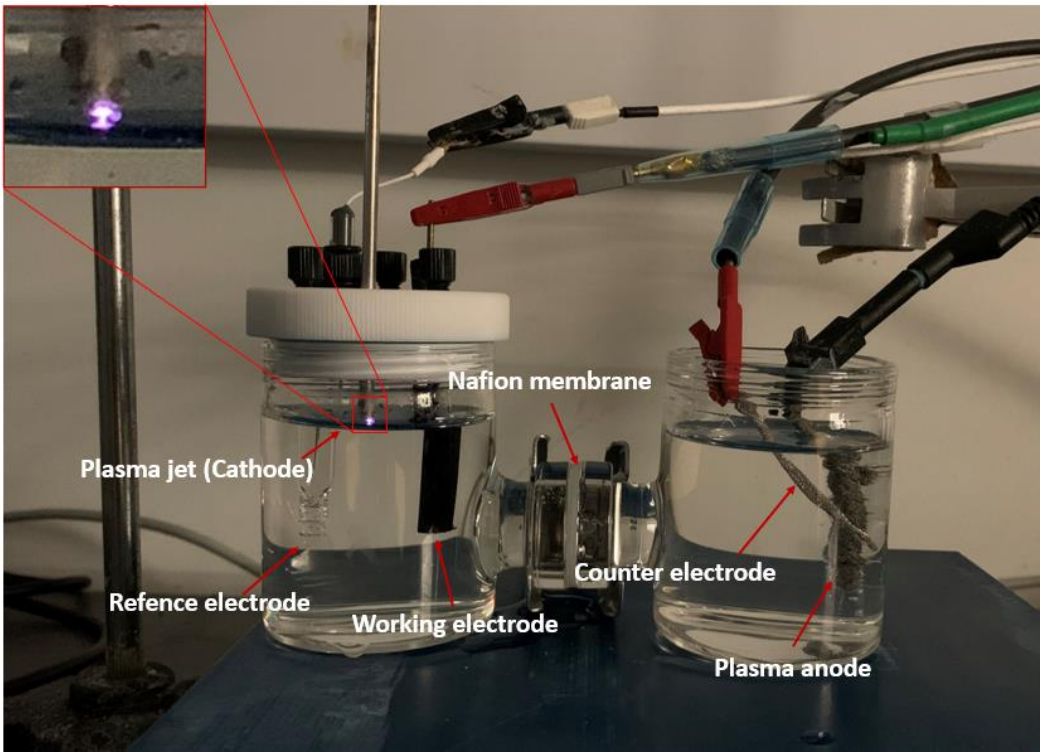

Figure 2. The experimental setup of the plasma-assisted electrochemical system. The reactor is an H-cell with two compartments separated by a Nafion membrane. The working electrode, i.e., a glassy carbon electrode coated with Pd catalysts, is submerged in an aqueous electrolyte, above which a micro plasma jet is ignited. The ignited plasma jet is shown in the inset.

For electrochemical tests without plasma discharge, the experiments were conducted following the standard electrochemical procedure. In electrochemical tests involving direct

current (DC) plasma, the plasma jet was connected to the negative pole of a high-voltage supply (PS325 2500 V; 25 W, Stanford Research Systems, Sunnyvale, CA, USA), relative to a submerged Pt electrode in the other chamber. The plasma was ignited at 2.5 kV, with a 274 kΩ ballast resistor limiting the plasma current. The left chamber's headspace was filled with Ar gas through the capillary tube at a flow rate of 30 sccm. Switching the polarity of the DC plasma involved connecting the capillary tube to the positive pole of the DC power supply, making the plasma jet the anode, and the Pt electrode connected to the negative pole as the cathode. For alternative current (AC)-driven nonthermal plasma electrochemical tests, the setup mirrored the DC-driven plasma, except the plasma jet was ignited by a high-voltage, high-frequency power supply (PVM/DDR plasma drive GME PM89 CLASS 2.5, Information Unlimited, Amherst, NH, USA) at 2.5 kV to achieve an AC plasma.

Before all electrochemical tests, CO_2 was sparged into a 0.5 M $KHCO_3$ solution for 30 min to achieve CO_2-saturated electrolyte. Subsequently, cyclic voltammetry (CV) and chronoamperometry tests were performed under various operating conditions (detailed in Tables 1–3). In the CV tests, the potential was scanned at 20 mV/s between −1.1 and 1 V vs. Ag/AgCl. The chronoamperometry tests were conducted at constant voltage of −0.92 V.

Table 1. The experiments conducted using Pd, 10% on carbon catalyst.

	Plasma Off	**Plasma Discharging Voltage**		**Plasma Operating Gas**		**Plasma Discharging Mode**		**Electrolysis Voltage**
		1.5 kV	**2.5 kV**	**Ar**	**CO_2**	**SIM [a]**	**SEP [b]**	**−0.92 V**
PdC1	×							×
PdC2			×		×	×		×
PdC3			×	×		×		×
PdC4			×		×		×	×
PdC5			×	×			×	×
PdC6		×		×		×		×
PdC7		×			×		×	×

×: applicable test condition. [a]: "SIM" is an abbreviation for "simultaneously". It indicates that electrochemical experiments are conducted at the same time as plasma discharge. [b]: "SEP" is an abbreviation for "separately". It indicates that the plasma discharge is conducted first, followed by electrochemical experiments.

Table 2. Experimental conditions for different plasma types.

	Without Plasma	**AC Plasma**	**DC Plasma**
	PdC1	**PdC8**	**PdC3**
Catalyst	Pd/C	Pd/C	Pd/C
Plasma discharging voltage	N/A	2.5 kV	2.5 kV
Plasma carrier gas	N/A	Ar	Ar
Plasma discharging mode	N/A	Simultaneously	Simultaneously
Anode	N/A	Plasma jet	Plasma jet
Cathode	N/A	Pt mesh	Pt mesh
Current type	N/A	AC	DC

Note: The condition "Without plasma" indicates that the electrochemical tests are conducted when the plasma is turned off. This is the control experiment, in which conventional electrochemical CO_2 reduction takes place. AC (alternative current) plasma and DC (direct current) plasma refer to the conditions when the electrochemical tests are performed under an AC plasma and a DC plasma, respectively. When either DC or AC plasma are utilized, the electrochemical tests are conducted simultaneously (at the same time) with plasma discharging. N/A means that the information is not available.

Table 3. The experimental conditions for different plasma voltage polarity conditions.

	Without Plasma	**Plasma as Anode**	**Plasma as Cathode**
	PdC1	**PdC9**	**PdC3**
Catalyst	Pd/C	Pd/C	Pd/C
Plasma discharging voltage	N/A	2.5 kV	2.5 kV
Plasma carrier gas	N/A	Ar	Ar
Plasma discharging mode	N/A	Simultaneously	Simultaneously
Anode	N/A	Plasma jet	Pt mesh
Cathode	N/A	Pt mesh	Plasma jet
Current type	N/A	DC	DC

Note: Without plasma means that electrochemical tests are conducted when the plasma is turned off. Plasma as anode denotes the test conditions when the electrochemical tests are performed with the plasma jet as the anode, and Plasma as cathode represents that the plasma jet is the cathode during electrochemical tests. Either plasma as the anode or as the cathode can be achieved by switching the polarity of the DC voltage generated by the high-voltage generator. N/A means that the information is not available. This happens when the plasma is turned off. Simultaneously means when the electrochemical tests are conducted at the same time as plasma discharging.

2.4. Quantitative Analysis of Formate

To quantify formate yield, chronoamperometry tests were conducted in a CO_2-saturated 0.5 M $KHCO_3$ electrolyte, with the applied voltage varying as indicated in Table 1. The tests lasted for 1 h. Following the tests, the electrolyte was collected and subjected to NMR analysis. In our prior work [14], we reported 1H-NMR spectra of the electrolyte. The NMR analysis was performed using a JEOL (Tokyo, Japan) 400 MHz spectrometer. The electrolyte was mixed with 100 µL of D_2O (99.9 atom % D, Sigma Aldrich, St. Louis, MO, USA) and 0.03 µL of dimethyl sulfoxide (99.9%, Sigma Aldrich, St. Louis, MO, USA). D_2O served for frequency locking, and DMSO acted as an internal reference and quantification standard. A distinctive peak of formate at the chemical shift of 8.2 ppm was observed, indicating formate as the primary CO_2RR product [11,12]. The obtained 1H-NMR spectra resemble those reported in the literature but lack other byproducts like phenols, suggesting potentially high selectivity toward formate in our electrochemical CO_2RR experiments.

We are interested in exploring conditions that could produce the most amount of formate. Thus, a precisely quantitative analysis of formate formation using NMR is essential. A calibration curve of formate concentration vs. formate peak intensity in the NMR spectra deserves to be established. To create such a curve, a series of standard formate solutions (0.010 mol/L, 0.017 mol/L, 0.037 mol/L, 0.071 mol/L, 0.086 mol/L, 0.111 mol/L, and 0.130 mol/L) were prepared, and then NMR analysis was performed. The intensity of the characteristic peak of formate at the chemical shift of 8.2 ppm was utilized to construct a calibration curve. After the calibration curve was established, a series of well-controlled chronoamperometry experiments were conducted. In those experiments, four factors, including plasma discharging voltage, plasma operating gas, and plasma discharging mode, were systematically varied, as shown in Tables 1–3.

2.5. Faradic Efficiency and Production Rate Calculation

To further quantify the influence of NTP on the formate formation at different testing conditions, the Faradic efficiency (*FE*) was calculated using the following equation:

$$FE_{formate} = \frac{n \times n_{formate} \times F}{\int_0^t Idt} \times 100\% \quad (1)$$

where $FE_{formate}$ is the faradic efficiency, n is the number of the transferred electrons when CO_2 is converted to formate and in this study n = 2, $n_{formate}$ is the amount (in moles) of the produced formate, F is the Faraday's constant, which is 96,485 C mole^{-1}, I is the electrochemical current, and t is the electrolysis time (s). The production rate (R) can be calculated from Equation (2):

$$R = \frac{n_{formate}}{t} \quad (2)$$

where the R is the production rate (moles/h); t is the time of electrolysis experiment.

3. Results and Discussions

Our previous studies indicate that the effectiveness of plasma in assisting CO_2RR is involved with multiple parameters (e.g., plasma discharging voltage, carrier gas, plasma discharging mode, etc.) [13,14]. To study the impact of those parameters, we conducted a series of comprehensive experiments in Tables 1–3. Those experiments were all performed in an H-shaped reactor (shown in Figures 1 and 2).

3.1. Impact of Plasma on CO_2RR

To investigate the impact of plasma discharge on electrochemical CO_2RR, cyclic voltammetry (CV) was performed in a 0.5 M $KHCO_3$ solution under three different conditions: without saturated CO_2 and plasma, with saturated CO_2 and no plasma, and with saturated CO_2 and plasma. Figure 3 presents the CV curves from −1.1 V to 1.0 V vs. Ag/AgCl. In the absence of CO_2 and plasma discharge, only the reduction peak corresponding to hydrogen evolution was observed (grey solid line in Figure 3). Upon purging CO_2 into the electrolyte for 30 min, an additional reduction peak at −0.92 V emerged, indicating the CO_2 reduction reaction (red and pink lines in Figure 3). However, this reduction peak appeared to shrink with increasing CV cycles, as shown in four consecutive CV scans. Two oxidation peaks at ~−0.51 V and 0 V appeared, possibly due to the oxidation of CO_2RR intermediates.

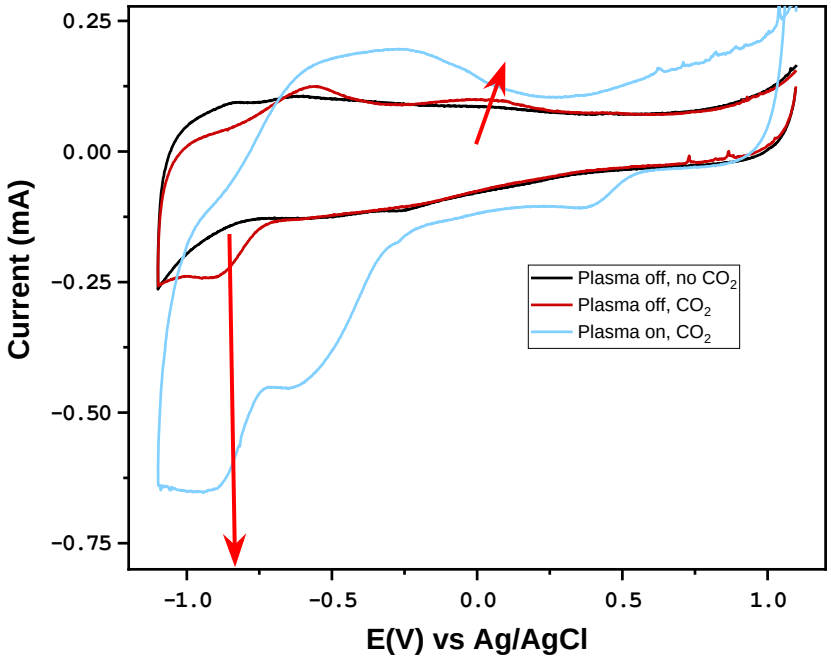

Figure 3. Cyclic voltammetry test results using Pd, 10 wt% on carbon catalyst. The experiments were conducted in a 0.5 M $KHCO_3$ solution with and without the presence of saturated CO_2 and DC plasma discharge.

To assess the impact of plasma on CO_2RR, the nonthermal plasma was ignited above the aqueous electrolyte immediately after the previous CV tests. Upon turning on the plasma discharge, we observed a drastic expansion of the cyclic voltammograms, i.e., the oxidation and reductions peaks augment in the direction, as indicated by the arrows shown in Figure 3. Particularly, the CO_2RR peak at −0.92 V was greatly enhanced, suggesting that nonthermal plasma discharge facilitates electrochemical CO_2RR. It is widely acknowledged that CO formation is inevitable during CO_2RR [11,12]. The formed CO, which is bonded

to the surface of the catalyst, blocks the active catalytic sites and diminishes the activity, resulting in low CO_2RR performance, as demonstrated by the attenuated reduction peak at −0.92 V in the presence of CO_2 but without plasma discharge. As discussed in the previous and a wealth of studies, such as reference [15], nonthermal plasma discharge above an aqueous solution produces H_2O_2. In our discovery, the formed H_2O_2 by the nonthermal plasma discharge appears to be beneficial for electrochemical CO_2RR, possibly owing to CO oxidation from the catalyst surface by the plasma-generated H_2O_2, therefore leading to more active catalytic sites for CO_2RR. The capability of the nonthermal plasma discharge on the adsorbate removal and catalyst activation is corroborated by the nearly 2× enhancement in CO_2 reduction current at −0.92 V. Recognizing that a voltage of −0.92 V is favorable for CO_2 reduction, subsequent experiments used this specific electrolysis voltage. The electrolysis voltage refers to the applied voltage in the electrochemical CO_2RR tests. Comparison of the produced formate concentrations from a series of experiments using the 10 wt% Pd/C catalyst at electrolysis voltage −0.92 V is illustrated in Figure 4. The bar graph illustrates the formic acid concentration (measured in millimoles per liter, mM) under different test conditions. These conditions vary based on the plasma conditions, plasma operating gas, and discharge mode, which are labeled from PdC1 to PdC9 (as shown in Table 1). The electrolysis voltage used in these tests is −0.92 V. PdC1, in which electrochemical nitrogen reduction occurs, serving as the control in the experiments. PdC2, when both electrochemical reduction and plasma discharge were conducted simultaneously, results in the highest formic concentration. As we move from PdC2 to PdC9, the bars sequentially decrease in height, suggesting a reduction in formic acid concentration. This graph provides insights into how the formic acid concentration varies with different electrolysis conditions and will be discussed in further context.

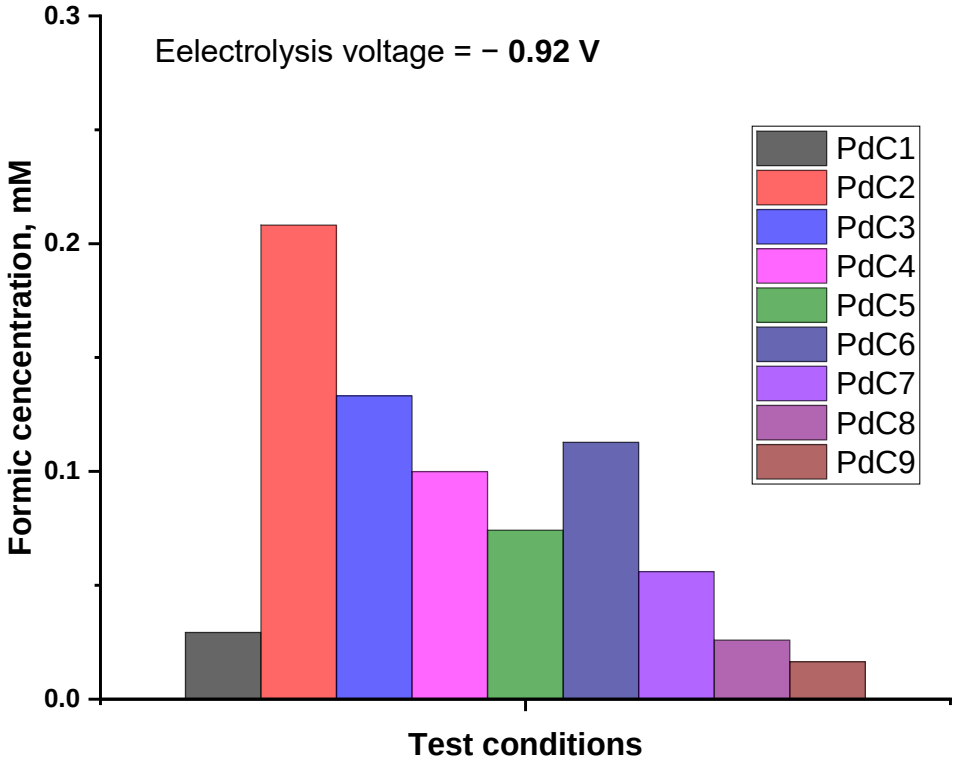

Figure 4. Comparison of the produced formate concentrations from a series of experiments listed in Tables 1–3. The concentration was determined using the characteristic peak of formate located at the chemical shift of 8.2 ppm in NMR spectra and the calibration curve.

3.2. Impact of Plasma Discharging Voltage

It is reported that plasma discharging voltage is critical to obtain energetic electrons at different energy levels [16] in a nonthermal plasma jet. Those energetic electrons are

vital to generate hydrated electrons upon entering the liquid, producing hydroxyl radicals and H_2O_2 [17] that is responsible for removing the adsorbed CO from the Pd catalyst surface. The comparison of plasma discharging voltage effect on the formate production is illustrated in Figure 5. Compared to other cases, the CO_2RR experiment in the absence of plasma (i.e., PdC1) yields the lowest formate concentration, suggesting that the CO_2 reduction by electrochemical process without plasma discharge is ineffective.

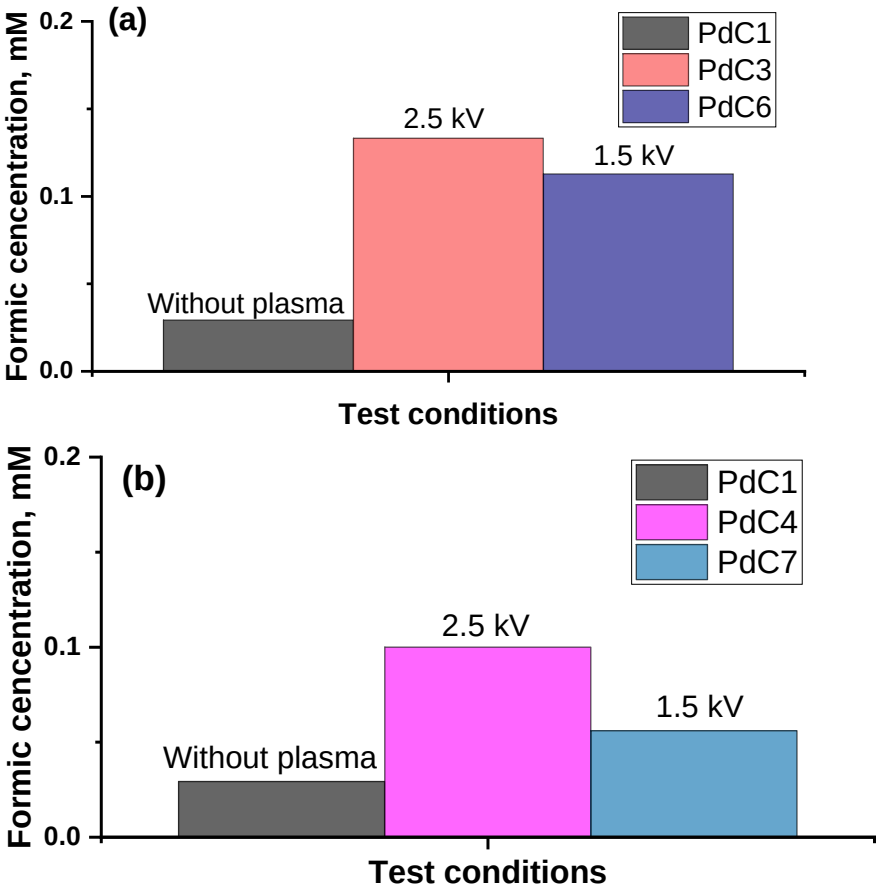

Figure 5. The effect of plasma discharging voltage on the produced formate concentrations from a series of experiments listed in Table 1 under different plasma discharging mode: (**a**) SIM and (**b**) SEP.

When the plasma operates at 1.5 kV (PdC6 and PdC7), it yields a higher formate production than the condition without plasma (PdC1, in the absence of plasma discharge). In addition, with an increase in plasma discharging voltage to 2.5 kV (PdC3 and PdC4), the concentration of formate production surpasses that observed at 1.5 kV (PdC6 and PdC7). This difference is attributed to the elevated plasma discharging voltage, leading to a greater generation of high-energy electrons within the electrochemical system. These electrons play a crucial role in the production of hydroxyl radicals and H_2O_2, which could facilitate reactivation of the catalyst [13] and contribute to enhanced formate production. Furthermore, a comparison between Figure 5a,b at identical plasma discharge voltages reveals that when electrochemical CO_2RR and plasma discharge occur simultaneously (SIM), CO_2 reduction to formate is enhanced compared to when they occur separately (SEP, i.e., in sequence). This observation strongly implies a synergistic effect between plasma discharge and electrochemical CO_2RR, a phenomenon that will be further explored in subsequent investigations.

3.3. Impact of Plasma Carrier Gas

Plasma carrier gas is employed to generate the plasma discharge. In this study, high DC voltages (2.5 kV and 1.5 kV) were applied beyond the dielectric limit of the operating

gas, inducing electrical breakdown. During this stage, the gas undergoes a transition from insulator to conductor as it becomes increasingly ionized. Various gases are used in plasma science, including Ar, He, Ne, H_2, N_2, etc. In this work, two operating gases (Ar or CO_2) were investigated. CO_2 served as both the carrier gas and the source of CO_2 to compensate for its loss in the electrolyte during electrochemical CO_2RR. Additionally, when used as the carrier gas, CO_2 may undergo vibrational excitation by the plasma, potentially leading to enhanced electrochemical CO_2RR by reducing the activation barrier.

Figure 6 illustrates the comparison of formate production using different plasma carrier gases (CO_2 and Ar). In comparison to both CO_2 and Ar as the plasma carrier gas, the formate concentration produced under nonplasma conditions (PdC1, in the absence of plasma discharge) is the lowest. When the plasma was activated with Ar as the carrier gas (PdC3), the produced formic concentration was higher than that of the nonplasma condition. Furthermore, upon switching the carrier gas to CO_2 (PdC2), the Pd/C catalysts produced at least 36% more formate than their counterparts when Ar was used as the carrier gas at −0.92 V (Figure 6a). Similarly, when the electrochemical tests were conducted after plasma discharging (also referred to as "SEP" in Table 1), the concentration of formate produced with CO_2 as the carrier gas (PdC4) remained higher than with Ar as the carrier gas (PdC5) (Figure 6b). The observed enhancement using CO_2 as the carrier gas might diminish due to the less-negative voltage (resulting in less electrochemical driving force for CO_2RR) and unoptimized electrochemical conditions. Nevertheless, CO_2 molecules in the carrier gas are easily activated under nonthermal plasma discharging conditions. Additionally, plasma could facilitate the transport of CO_2 molecules in the liquid electrolyte, making them largely available at the Pd catalysts.

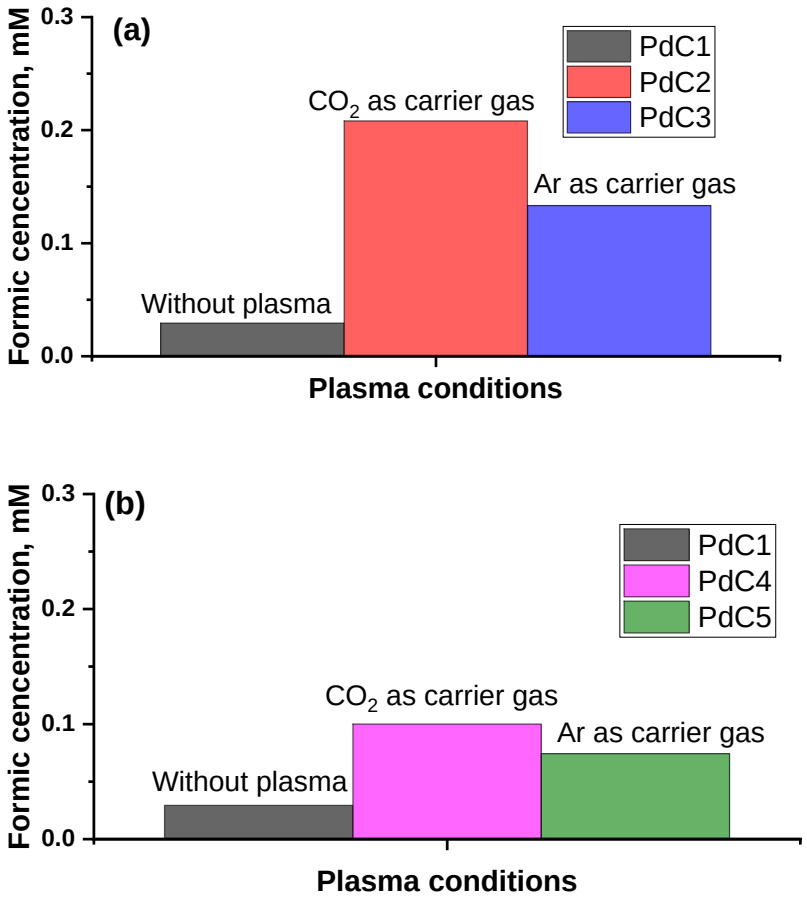

Figure 6. The effect of plasma carrier gas on the produced formate concentrations from a series of experiments listed in Table 1 under different plasma discharging mode: (**a**) SIM and (**b**) SEP.

3.4. Impact of Plasma Discharging Mode

This study investigates two different plasma discharging modes: simultaneous (SIM) plasma discharging and separate (SEP) plasma discharging. In SIM plasma discharging, plasma discharging occurs simultaneously with the electrochemical tests, while SEP plasma discharging involves conducting plasma discharging first, followed by the electrochemical tests. Figure 7 compares the formate concentrations using Pd/C using different plasma supply gases (CO_2 and Ar). When the plasma supply gas was CO_2 (Figure 7a), the concentration of formate produced by SIM plasma (PdC2) was higher than SEP plasma (PdC4). If the plasma was turned off (PdC1), the produced formate concentration was the lowest, as seen in Figure 7a. A similar pattern was observed when Ar was used as the plasma supply gas (Figure 7b), where SIM plasma (PdC3) resulted in the highest formate production, followed by SEP plasma (PdC5) and, finally, the condition without plasma discharging (PdC1).

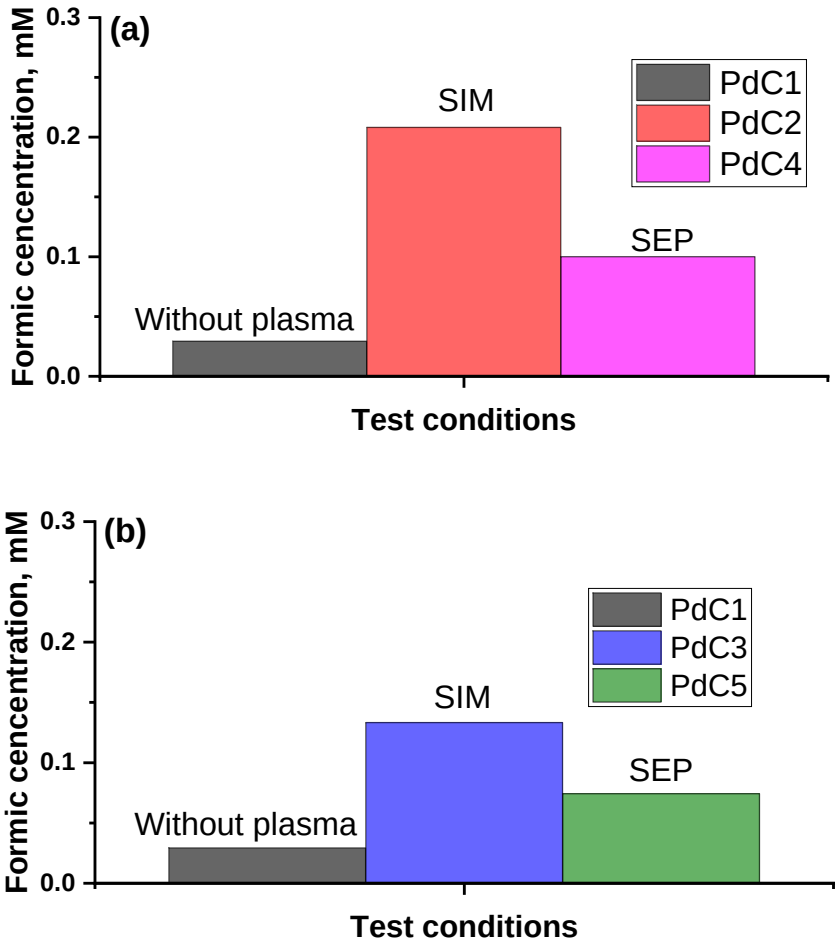

Figure 7. The effect of plasma discharging mode (2.5 kV) on the produced formate concentrations from a series of experiments listed in Table 1 using different plasma carrier gas: (**a**) CO_2 and (**b**) Ar. Three different plasma discharge modes are studied: SEP, SIM, and without plasma, i.e., with the absence of plasma discharge.

Whether at high (2.5 kV) or low (1.5 kV) plasma discharging voltage, SIM plasma is more effective in producing formate compared to SEP plasma. This is attributed to the reactive species generated by plasma. Reactive species produced by nonthermal plasma are short-lived and tend to react with water or other molecules in the electrolyte. During SIM plasma discharging, reactive species are continually produced, promoting the formation of H_2O_2 and assisting CO_2RR. Switching to SEP plasma discharging, reactive species also facilitate the formation of large amounts of H_2O_2. By the time SEP plasma discharging

finishes, the H_2O_2 concentration reaches a plateau. However, after SEP plasma discharge, H_2O_2 is gradually consumed by the electrochemical test, and no more H_2O_2 is supplied to the electrolyte to promote CO_2RR. The Pd/C catalyst's active surface is likely blocked by the byproduct (mainly CO) of CO_2RR, leading to catalyst deactivation. As more CO is produced from electrochemical tests, the catalyst's activity keeps declining, resulting in a lower formate concentration.

3.5. Impact of Plasma Type

Typically, nonthermal direct current (DC) plasma is characterized by low voltage and high current density. Conversely, high-frequency alternative current (AC) plasma is produced by an AC power supply with rapidly changing polarity. To investigate the impact of plasma type on electrochemical formate production, CV and chronoamperometry tests were conducted under three conditions: with a DC plasma, an AC plasma, or no plasma. The condition without plasma represents the conventional electrochemical CO_2RR, where the plasma is deactivated during electrochemical tests. In contrast, the AC and DC plasmas are generated using high AC and DC voltages, respectively. The specific experimental conditions are detailed in Table 2.

Figure 8 presents a comparison of CV curves under three different plasma conditions: without plasma discharging (dash curve), AC plasma discharging, and DC plasma discharging. In comparison to the condition without plasma (red dash curve) and DC plasma (blue dotted curve), both the reduction and oxidation peaks in the CV curves diminish after turning on the AC plasma. Specifically, the current of the reduction peak at −1.0 V reduces by 3.4 times upon activating the AC plasma, indicating the suppression of the electrochemical behavior of the Pd electrode in the aqueous electrolyte. Conversely, for the oxidation peak at −0.5 V, the current intensity without plasma is 4.05 times higher than that with AC plasma. In contrast, immediately after turning on the DC plasma, the CV curve experiences a significant enhancement. The current intensity for the reduction peak at −1.0 V is 4.43 times higher with the presence of DC plasma compared to AC plasma. Similarly, the oxidation peak at −0.5 V is 10.34 times stronger than that with AC plasma. When comparing the three plasma conditions, it is notable that the CV curves with AC plasma are not smooth, displaying high-frequency current fluctuations with changing electrolysis voltage. This behavior is attributed to the intrinsic nature of AC plasma, which periodically reverses direction and continuously changes its amplitude over time. Consequently, the AC voltage affects the stability of plasma discharging above the electrolyte, influencing the smoothness of the CV curves.

Figure 9 depicts a comparison of chronoamperometry tests conducted at −0.92 V vs. Ag/AgCl under different plasma conditions, including without plasma, AC plasma, and DC plasma. Consistent with the CV results, the electrochemical CO_2RR under −0.92 V with AC plasma exhibits a significantly smaller current. Upon activating the AC plasma, the electrochemical CO_2RR current decreases sharply by 10 times, dropping from −0.1 mA to around −0.01 mA. In contrast, the electrochemical CO_2RR current in the presence of DC plasma gradually declines from −0.16 mA to around −0.025 mA. These findings suggest that the electrochemical CO_2 reduction performance benefits from DC plasma discharge, while AC plasma appears to have a negative impact, possibly arising from diminished electrochemical active surface area evidenced from Figure 8.

Following the electrochemical test, the electrolyte was collected for NMR analysis, and the formate concentration was calculated. Figure 10 illustrates the formate concentrations in the electrolyte after the electrochemical CO_2RR tests under three conditions: without plasma discharge, with high-frequency AC plasma, and with DC plasma. The results clearly show that DC plasma generated the highest amount of formate, with a concentration of 0.133 mM. In contrast, the formate concentration produced by AC plasma is only 0.025 mM, which is 5.32 times less than that of DC plasma. Surprisingly, compared to the test without plasma discharging, the formate concentration produced with AC plasma is even smaller, by −0.003 mM. These results further validate the observation that plasma conditions

significantly impact electrochemical performance, with nonthermal DC plasma proving the most effective among the three conditions.

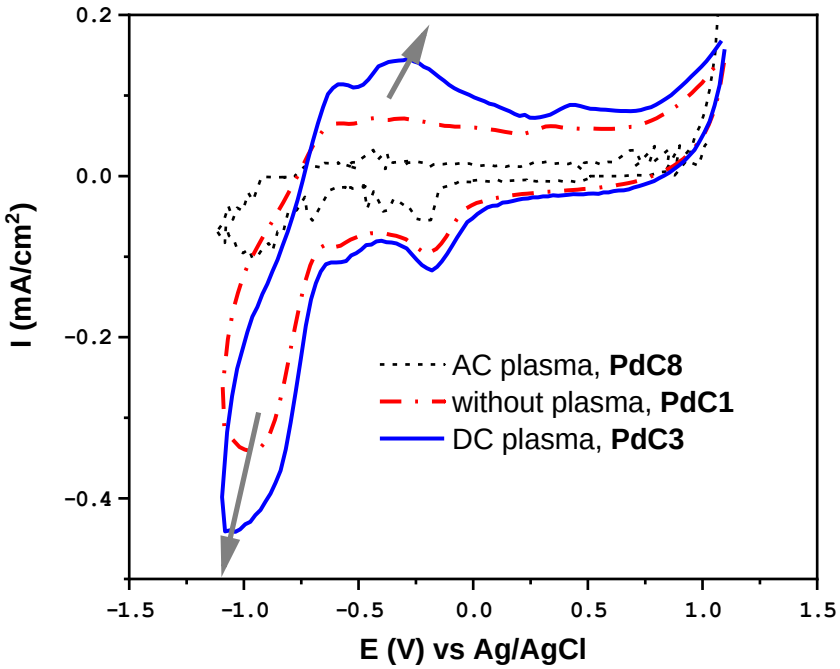

Figure 8. The comparison of CV curves for plasma electrochemical CO_2RR at three different conditions (PdC1, PdC3, and PdC8): AC plasma, DC plasma, and in the absence of plasma. A 2.5 kV discharging voltage, simultaneously discharging mode, Ar gas, and Pd/C, were used in the experiments.

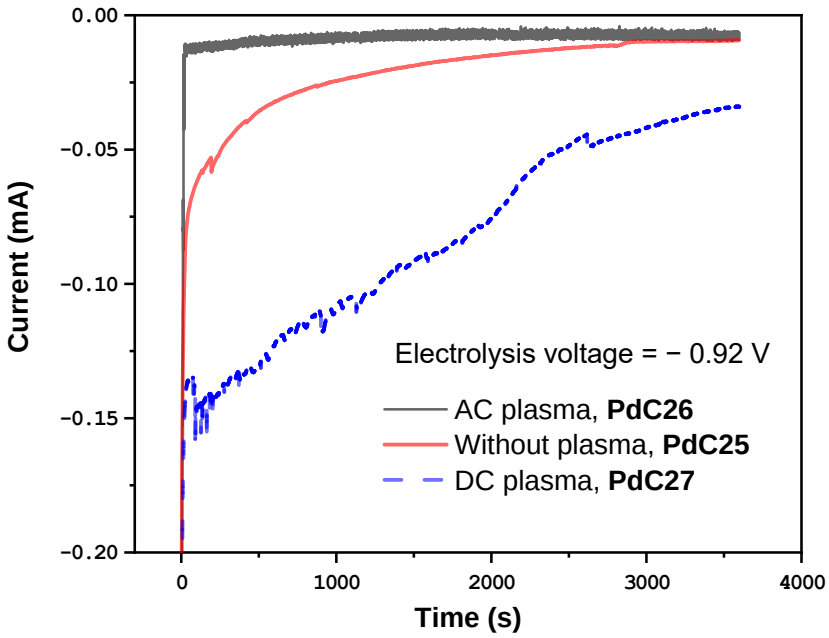

Figure 9. The chronoamperometry test results for plasma electrochemical CO_2RR at three different plasma conditions (PdC1, PdC3, and PdC8): AC plasma, DC plasma, and in the absence of plasma. A 2.5 kV discharging voltage, simultaneously discharging mode, Ar gas, Pd/C, and −0.92 V vs. Ag/AgCl electrolysis voltage, were used in the experiments.

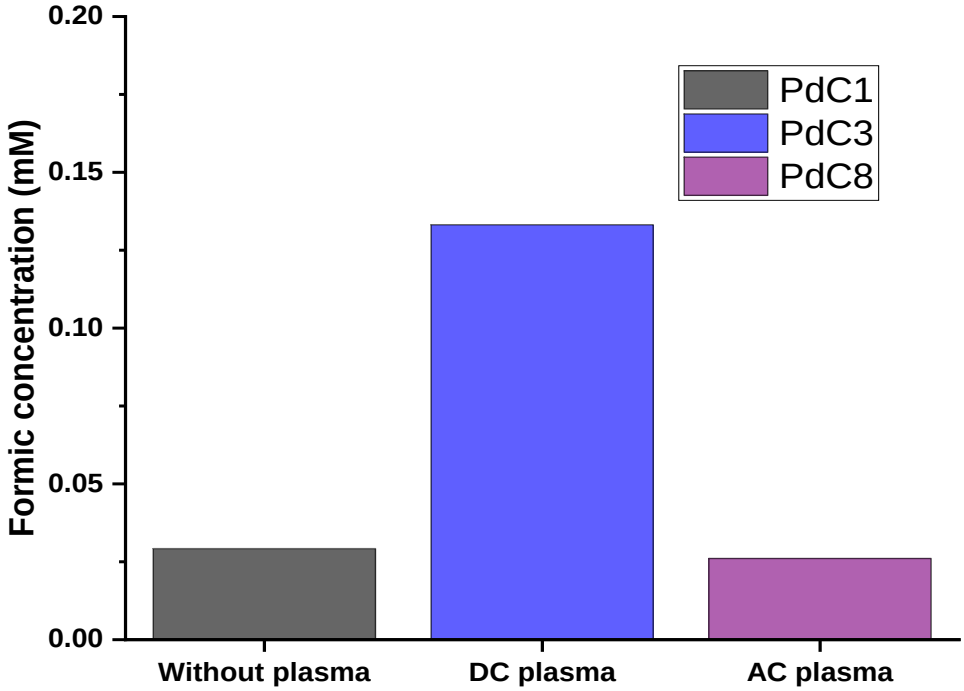

Figure 10. The effect of plasma discharging type on the produced formate concentrations from a series of experiments listed in Table 2. The concentration was determined using the characteristic peak of formate located at the chemical shift of 8.2 ppm in NMR spectra and the calibration curve.

In the context of AC plasma liquid interaction, the gas temperature can reach higher levels than in DC plasma [18]. Despite being labeled nonthermal, the AC plasma used in this work still exhibits temperature elevation [19]. The accumulated heat in the reactor could lead to electrolyte evaporation, evident by fog and condensation observed on the reactor wall after a few minutes of AC plasma discharging. Additionally, it is reported that formate and H_2O_2 are prone to decomposition at high temperatures [20,21]. Thus, employing AC plasma in assisting electrochemical CO_2RR may lead to the decomposition of formate and H_2O_2, hindering catalyst activities and resulting in lower formate formation through AC plasma.

3.6. Impact of Switching Plasma Polarity

Numerous published studies highlight the significance of intrinsic electrical properties of plasma, such as current type (DC or AC) and polarity (plasma jet as the anode or cathode), in influencing both charged and chemical species generation [22,23]. Specifically, the difference between AC and DC plasma lies in their generation mechanisms. DC plasma operates by ionizing a carrier gas between two electrodes with a sufficiently high potential, leading to electron acceleration from the cathode towards the liquid electrolyte and ionized species from the anode towards the electrolyte. In contrast, AC plasma requires an AC power source, and the directions of electrons and ionized species switch at a high frequency (usually in the RF range of 10–14 MHz). To explore the impact of switching plasma polarity, comprehensive experiments were conducted under different conditions, as outlined in Table 3.

Figure 11 presents CV curves obtained under various conditions, including electrochemical CO_2RR in the absence of plasma discharge (PdC1), DC plasma as the anode (PdC9), or as the cathode (PdC3). A comparison of CV curves with different plasma voltage polarities reveals that the CO_2 reduction peak (−1.0 V vs. Ag/AgCl) becomes barely noticeable when the nonthermal anode plasma jet is used alongside electrochemical CO_2RR, indicating significant suppression of CO_2RR activity. Upon switching plasma polarity (i.e., the plasma jet becomes the cathode), CO_2RR peaks reappear. On the other hand, hydrogen evolution (−1.1~−0.75 V vs. Ag/AgCl) with plasma as the anode is notably enhanced and the maximum current intensity is around 11 times higher than that with plasma as the cathode. However, this enhancement in hydrogen evolution unavoidably undermines the rate and efficiency of CO_2 reduction.

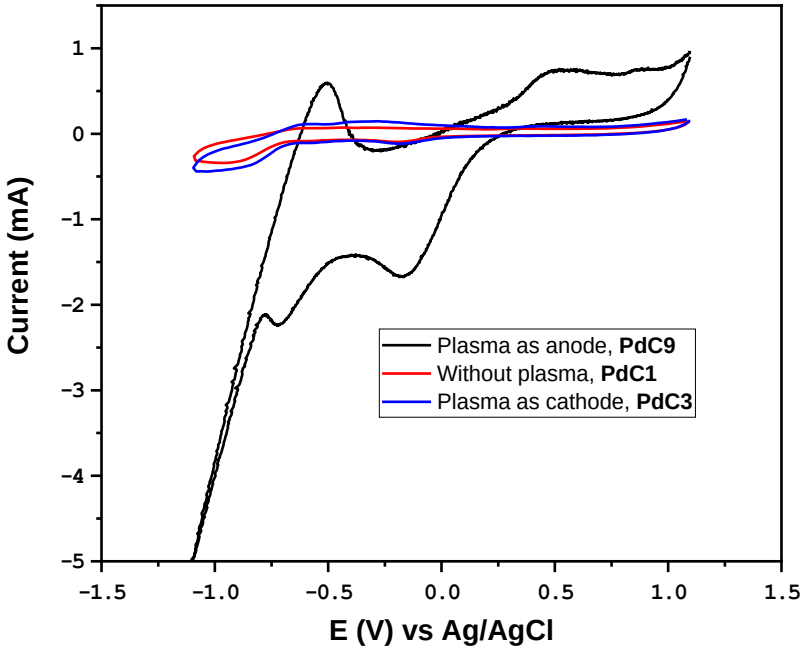

Figure 11. The comparison of CV curves for plasma electrochemical CO_2RR at three different conditions (PdC1, PdC3, and PdC9). A 2.5 kV discharging voltage, simultaneously discharging mode, Ar gas, and Pd/C, were used in the experiments.

Figure 12 compares chronoamperometry tests for three different voltage polarities (without plasma, plasma as anode, and plasma as cathode). It is evident that when the nonthermal plasma jet serves as the anode, the current obtained is significantly higher than values achieved without plasma or with plasma as the cathode. The maximum current obtained when plasma serves as the anode is almost 75 times higher than when it serves as the cathode. Additionally, the electrolytes after chronoamperometry tests were collected and analyzed. Figure 13 illustrates the comparison of formate concentrations under three different plasma voltage polarity conditions. The plasma cathode (PdC3) produces the highest formate concentration, followed by the test in the absence of plasma discharge, and then the plasma anode. Compared to the nonthermal plasma serving as the anode, the formate concentration produced when it serves as the cathode is 7.9 times higher. Even in the absence of plasma discharging, the concentration of formate produced from electrochemical CO_2RR is still higher, providing further evidence that the plasma anode is not conducive to electrochemical CO_2RR. All the above test results consistently indicate that the plasma anode is not favorable for electrochemical CO_2RR.

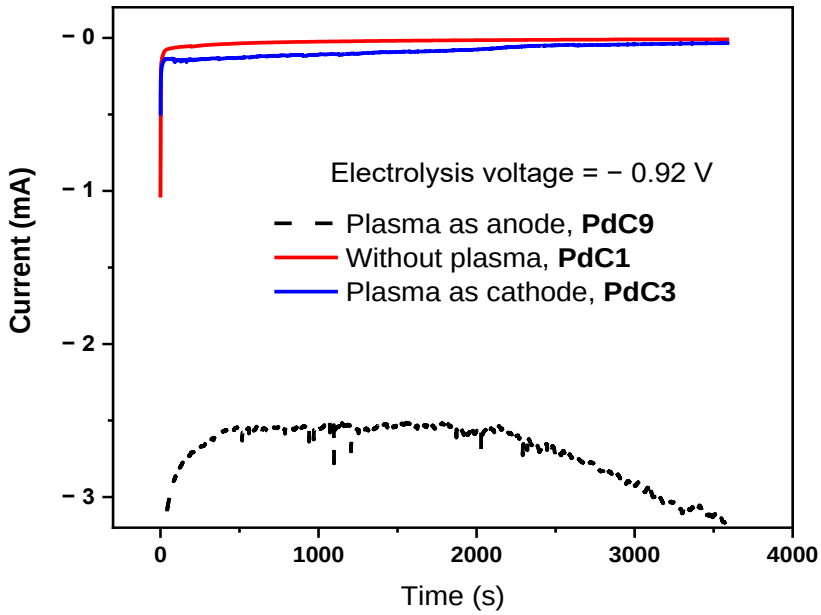

Figure 12. Chronoamperometry test results for plasma electrochemical CO_2RR at three different conditions (PdC1, PdC3, and PdC9). A 2.5 kV discharging voltage, Ar gas as the plasma supply gas, Pd/C, and −0.92V vs. Ag/AgCl electrolysis voltage were used in the experiments.

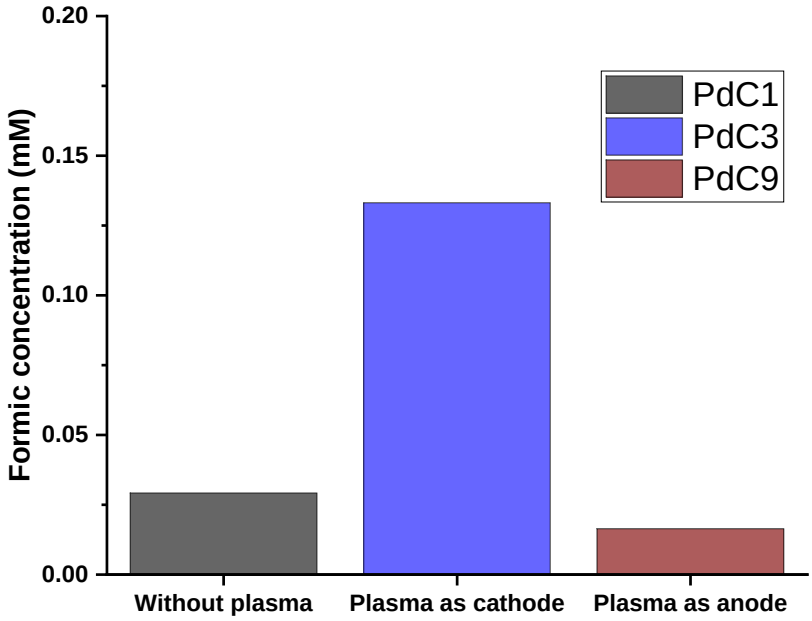

Figure 13. The effect of switching plasma polarity on the produced formate concentrations from a series of experiments listed in Table 3.

3.7. Faradic Efficiency and Production Rate

The production rates and faradic efficiency ($FE_{formate}$) of the tests are detailed in Table 4. The highest $FE_{formate}$, reaching 23.52%, was observed in the test utilizing high plasma voltage at 2.5 kV, CO_2 as the carrier gas, 10 wt% Pd on carbon catalyst, and SEP mode (PdC4). The elevated plasma discharging facilitated the generation of more energy-reactive species, promoting CO_2RR and enhancing $FE_{formate}$. While some plasma-generated reactive species are short-lived and prone to decomposition or reactions with other compounds or molecules [16], long-lived H_2O_2 from nonthermal plasma discharge fosters CO_2RR. Surprisingly, the highest formate concentration was achieved under the condition of high plasma voltage at 2.5 kV, CO_2 as the carrier gas, 10 wt% Pd on carbon

catalyst, and SIM mode (PdC2). This suggests that a higher formate concentration does not necessarily equate to a higher formate faradic efficiency.

Table 4. Faradic efficiency and production rate of formate at different conditions for Pd, on 10% carbon catalyst.

Experiment Conditions	$FE_{formate}$	Production Rate (mole/h)
PdC1	2.87%	7.034×10^{-9}
PdC2	4.87%	1.697×10^{-8}
PdC3	8.10%	2.975×10^{-8}
PdC4	23.52%	3.925×10^{-8}
PdC5	17.60%	5.571×10^{-8}
PdC6	11.21%	6.389×10^{-8}
PdC7	8.60%	1.443×10^{-8}
PdC8	7.88%	1.300×10^{-8}
PdC9	0.016%	8.195×10^{-9}

The $FE_{formate}$ under three different plasma voltage polarity conditions (PdC1, PdC3, and PdC9) is also presented in Table 4. Under the SIM mode, the maximum $FE_{formate}$ is achieved when the nonthermal plasma serves as the cathode (PdC3) and can reach as high as 8.1%. In contrast, the $FE_{formate}$ is less than 1% when the nonthermal plasma jet serves as the anode (PdC9). As indicated in Equation (1), the calculation of $FE_{formate}$ involves several parameters, including the number of transferred electrons when CO_2 is converted to formate and the amount of produced formate, among others. Figures 11 and 12 suggest that substantial parasitic reactions, such as hydrogen evolution or oxygen reduction, occur when the nonthermal plasma jet serves as the anode. However, when comparing electrochemical CO_2RR tests with or without the presence of the plasma cathode, the concentration of formate produced when the nonthermal plasma serves as the anode is barely notable (Table 4, PdC9). Even with plenty of electrons flowing through the electrochemical system, the majority of them contribute to massive hydrogen evolution or oxygen reduction. Additionally, electrochemical CO_2RR does produce formate. Regarding the formate production rate, when the nonthermal jet serves as the cathode (Table 4, PdC3), electrochemical CO_2RR produces 8.12 times more formate than when using plasma as the anode.

The obtained faradaic efficiencies in Table 4 are slightly lower than reported values in the literature, which typically range from 35% to 90% when electrochemical CO_2 reduction is conducted at high pressure [24] or using a two-compartment flow cell [25]. The obtained formate production rates are also lower. However, under similar experimental setup, the highest FE achieved in Table 4 (FE = 23.52%) surpasses values obtained at 1 atm CO_2 pressure (FE = 3.52%) and even at 9 atm (FE = 20.8%) reported in reference [26].

The power consumption of our plasma electrochemical system is significantly higher (2~3 times larger) compared to that of electrochemical CO_2RR, primarily attributed to the added energy demand from plasma discharge. Nonetheless, exploring modifications such as adjusting electrode geometry or exploring the use of AC plasma instead of the DC plasma utilized in this study holds promise for integrating the system with renewable energy sources. This is particularly noteworthy as the costs associated with renewable energy are consistently decreasing. With further exploration and optimization, the approach presented here could become a potentially promising technology for green, economical CO_2 production.

4. Conclusions

In conclusion, this study investigates the intricate effect of nonthermal plasma (NTP)-assisted electrochemical reduction of CO_2, focusing on the production of formate ($HCOO^-$ / HCOOH) as a valuable end product. The research systematically explores various factors influencing NTP-assisted electrochemical CO_2 reduction, including plasma discharging

voltage, carrier gas, discharging mode, polarity, and plasma type. Experimental results demonstrate that NTP discharge significantly enhances formate production compared to conventional electrochemical processes. The impact of parameters such as voltage, carrier gas, and discharging mode is thoroughly investigated, providing valuable insights into optimizing conditions for efficient formate synthesis. Moreover, the study elucidates the advantage of nonthermal DC plasma over AC plasma, emphasizing its positive influence on electrochemical CO_2 reduction. The investigation into switching plasma polarity reveals that the plasma cathode significantly outperforms the plasma anode in terms of formate production. Faradic efficiency and production rate calculations underscore the effectiveness of NTP in promoting CO_2 reduction, with notable achievements in certain experimental conditions. The findings contribute valuable knowledge to the emerging field of NTP-assisted electrochemical CO_2 reduction, paving the way for sustainable solutions to mitigate rising CO_2 levels and address environmental concerns.

Author Contributions: J.H. carried out the experiment. J.H. and F.L. wrote the manuscript. All authors have read and agreed to the published version of the manuscript.

Funding: This study was funded by University of Massachusetts Lowell.

Institutional Review Board Statement: Not applicable.

Informed Consent Statement: Not applicable.

Data Availability Statement: Derived data supporting the findings of this study are available from the corresponding author on request.

Acknowledgments: We extend our gratitude to Snigdha Rashinkar for her valuable contribution in collecting some of the data reported in this work. We also acknowledge the support from the Department of Mechanical & Industrial Engineering at the University of Massachusetts Lowell.

Conflicts of Interest: The authors declare no conflict of interest.

References

1. Sun, D.; Xu, X.; Qin, Y.; Jiang, S.P.; Shao, Z. Rational Design of Ag-Based Catalysts for the Electrochemical CO_2 Reduction to CO: A Review. *ChemSusChem* **2020**, *13*, 39–58. [CrossRef] [PubMed]
2. Xiong, L.; Zhang, X.; Chen, L.; Deng, Z.; Han, S.; Chen, Y.; Zhong, J.; Sun, H.; Lian, Y.; Yang, B. Geometric Modulation of Local CO Flux in Ag@Cu_2O Nanoreactors for Steering the CO_2RR Pathway toward High-Efficacy Methane Production. *Adv. Mater.* **2021**, *33*, 2101741. [CrossRef] [PubMed]
3. Meng, D.L.; Zhang, M.D.; Si, D.H.; Mao, M.J.; Hou, Y.; Huang, Y.B.; Cao, R. Highly Selective Tandem Electroreduction of CO_2 to Ethylene over Atomically Isolated Nickel–Nitrogen Site/Copper Nanoparticle Catalysts. *Angew. Chem.* **2021**, *133*, 25689–25696. [CrossRef]
4. Leverick, G.; Bernhardt, E.M.; Ismail, A.I.; Law, J.H.; Arifutzzaman, A.; Aroua, M.K.; Gallant, B.M. Uncovering the Active Species in Amine-Mediated CO_2 Reduction to CO on Ag. *ACS Catal.* **2023**, *13*, 12322–12337. [CrossRef]
5. Fernández-Caso, K.; Díaz-Sainz, G.; Alvarez-Guerra, M.; Irabien, A. Electroreduction of CO_2: Advances in the Continuous Production of Formic Acid and Formate. *ACS Energy Lett.* **2023**, *8*, 1992–2024. [CrossRef]
6. Yang, H.; Wu, Y.; Li, G.; Lin, Q.; Hu, Q.; Zhang, Q.; Liu, J.; He, C. Scalable production of efficient single-atom copper decorated carbon membranes for CO_2 electroreduction to methanol. *J. Am. Chem. Soc.* **2019**, *141*, 12717–12723. [CrossRef] [PubMed]
7. Shen, H.; Jin, H.; Li, H.; Wang, H.; Duan, J.; Jiao, Y.; Qiao, S.-Z. Acidic CO_2-to-HCOOH electrolysis with industrial-level current on phase engineered tin sulfide. *Nat. Commun.* **2023**, *14*, 2843. [CrossRef] [PubMed]
8. Gao, D.; Zhou, H.; Cai, F.; Wang, J.; Wang, G.; Bao, X. Pd-containing nanostructures for electrochemical CO_2 reduction reaction. *ACS Catal.* **2018**, *8*, 1510–1519. [CrossRef]
9. Hori, Y.; Wakebe, H.; Tsukamoto, T.; Koga, O. Electrocatalytic process of CO selectivity in electrochemical reduction of CO_2 at metal electrodes in aqueous media. *Electrochim. Acta* **1994**, *39*, 1833–1839. [CrossRef]
10. Zhao, C.; Yin, Z.; Wang, J. Efficient Electrochemical Conversion of CO_2 to HCOOH Using Pd-polyaniline/CNT Nanohybrids Prepared in Situ. *ChemElectroChem* **2015**, *2*, 1974–1982. [CrossRef]
11. Min, X.; Kanan, M.W. Pd-catalyzed electrohydrogenation of carbon dioxide to formate: High mass activity at low overpotential and identification of the deactivation pathway. *J. Am. Chem. Soc.* **2015**, *137*, 4701–4708. [CrossRef] [PubMed]
12. Gao, D.; Zhou, H.; Cai, F.; Wang, D.; Hu, Y.; Jiang, B.; Cai, W.-B.; Chen, X.; Si, R.; Yang, F. Switchable CO_2 electroreduction via engineering active phases of Pd nanoparticles. *J. Nano Res.* **2017**, *10*, 2181–2191. [CrossRef]
13. Hu, J.; Lin, G.; Liu, F. Plasma-Assisted Catalyst Active Phase Regeneration in Formate-Selective Carbon Dioxide Electroreduction. In Proceedings of the Electrochemical Society Meeting Abstracts 237, Montreal, QC, Canada, 10–14 May 2020; p. 1116.

14. Hu, J. Non-Thermal Plasma Assisted Pd Catalyst Deactivation in Electrochemical CO_2 Reduction Reaction. Ph.D. Dissertation, Mechanical Engineering, University of Massachusetts Lowell, Lowell, MA, USA, 2022.
15. Locke, B.R.; Shih, K.-Y. Review of the methods to form hydrogen peroxide in electrical discharge plasma with liquid water. *Plasma Sources Sci. Technol.* **2011**, *20*, 034006. [CrossRef]
16. Bruggeman, P.; Kushner, M.J.; Locke, B.R.; Gardeniers, J.G.; Graham, W.; Graves, D.B.; Hofman-Caris, R.; Maric, D.; Reid, J.P.; Ceriani, E. Plasma–liquid interactions: A review and roadmap. *Plasma Sources Sci. Technol.* **2016**, *25*, 053002. [CrossRef]
17. Tian, W.; Kushner, M.J. Atmospheric pressure dielectric barrier discharges interacting with liquid covered tissue. *J. Phys. D Appl. Phys.* **2014**, *47*, 165201. [CrossRef]
18. Li, J.; Wu, F.; Nie, L.; Lu, X. The effect of phase shift on the plasma driven by an AC voltage and a pulsed DC voltage. *IEEE Trans. Plasma Sci.* **2019**, *47*, 4818–4826. [CrossRef]
19. Pang, Y.; Hammer, T.; Müller, D.; Karl, J. Investigation on the influence of non-thermal plasma on reaction degree of wood gasification in a drop tube reactor. *Fuel* **2019**, *253*, 95–105. [CrossRef]
20. Pędziwiatr, P. Decomposition of hydrogen peroxide-kinetics and review of chosen catalysts. *Acta Innov.* **2018**, 45–52. [CrossRef]
21. Bahuguna, A.; Sasson, Y. Formate-Bicarbonate Cycle as a Vehicle for Hydrogen and Energy Storage. *ChemSusChem* **2021**, *14*, 1258–1283. [CrossRef]
22. Rumbach, P.; Xu, R.; Go, D.B. Electrochemical production of oxalate and formate from CO_2 by solvated electrons produced using an atmospheric-pressure plasma. *J. Electrochem. Soc.* **2016**, *163*, F1157. [CrossRef]
23. Lee, H.; Lee, C.-H.; Choi, J.-W.; Song, H.K. The effect of the electric pulse polarity on CO_2 reforming of CH_4 using dielectric barrier discharge. *Energy Fuels* **2007**, *21*, 23–29. [CrossRef]
24. Scialdone, O.; Galia, A.; Nero, G.L.; Proietto, F.; Sabatino, S.; Schiavo, B. Electrochemical reduction of carbon dioxide to formic acid at a tin cathode in divided and undivided cells: Effect of carbon dioxide pressure and other operating parameters. *Electrochim. Acta* **2016**, *199*, 332–341. [CrossRef]
25. Natsui, K.; Iwakawa, H.; Ikemiya, N.; Nakata, K.; Einaga, Y. Stable and Highly Efficient Electrochemical Production of Formic Acid from Carbon Dioxide Using Diamond Electrodes. *Angew. Chem. Int. Ed.* **2018**, *57*, 2639–2643. [CrossRef] [PubMed]
26. Kas, R.; Kortlever, R.; Yılmaz, H.; Koper, M.T.M.; Mul, G. Manipulating the Hydrocarbon Selectivity of Copper Nanoparticles in CO_2 Electroreduction by Process Conditions. *ChemElectroChem* **2015**, *2*, 354–358. [CrossRef]